Effects of normalisation and mild-slope approximation on wave reflection by bathymetry in a Hamiltonian wave model

Maarten W. Dingemans[1] **and Gert Klopman**[2]

[1] **Boomkensdiep 11, 8303 KW Emmeloord, The Netherlands, e-mail: maarten.dingemans@deltares.nl**
[2] **Albatros Flow Research, Zwolle, The Netherlands, e-mail: g.klopman@afr.nl**

Introduction Wave reflection by sea bed topography often poses a strong challenge to the performance characteristics of a wave model. While many wave models obtain quite accurate results with respect to wave shoaling, refraction and diffraction, not so much perform well with respect to wave reflection by sea-bed changes. Here, we will study the wave reflection characteristics of a Hamiltonian wave model with a Boussinesq-like approach to the approximation of the vertical structure of the flow (Klopman *et al.*, 2005, 2007). We will do this for linear waves propagating in one horizontal dimension. The Hamiltonian is the sum of the kinetic and potential energies of the flow. In the Hamiltonian the integral of the kinetic energy density over depth is simplified by using an approximation for the shape of flow velocity profiles over depth. As a result, the Hamiltonian model only depends on horizontal position and time, and no longer on the vertical coordinate. To further simplify the resulting wave model, one may neglect the terms dependent on bed slope in the Hamiltonian, which results in a so-called mild-slope approximation. We compare the wave reflection results of the mild-slope variant of our model with the so-called steep-slope variant (with the bed-slope terms included). It is found that the steep-slope model is very accurate with respect to reflection, when comparing with highly-accurate numerical results of Porter & Porter (2006). On the other hand, the mild-slope model is not very accurate with respect to reflection.
During the course of our research, normalisation of the used vertical shape functions has been found to give a large effect on reflection characteristics. Because mild-slope models are of simpler form than the corresponding steep-slope variants, this tempted us to search for mild-slope models with optimised normalisation of the shape function. As a result, we are able to construct mild-slope models with reflection characteristics comparable in accuracy to the steep-slope model.

Hamiltonian model The Hamiltonian description of a free-surface potential flow was found by Zakharov (1968). The flow velocity is the gradient of the velocity potential $\Phi(\boldsymbol{x}, z, t)$, in a fluid domain bounded by the free surface at $z = \zeta(\boldsymbol{x}, t)$ and the sea bed at $z = -h(\boldsymbol{x})$, where h is the still-water depth. Under the action of the gravitational acceleration, acting in the negative z-direction, the Hamiltonian $\mathscr{H}$ is the sum of the kinetic and potential energies:

$$(1) \qquad \mathscr{H} = \iint \left\{ \int_{-h}^{\zeta} \frac{1}{2}\rho \left[|\boldsymbol{\nabla}\Phi|^2 + (\partial_z \Phi)^2 \right] \mathrm{d}z + \frac{1}{2}\rho\, g\, \zeta^2 \right\} \mathrm{d}\boldsymbol{x},$$

where $\boldsymbol{x}$ is the horizontal position vector, t is time and ρ is the fluid density (which is assumed to be a constant). The non-linear evolution of the surface elevation $z = \zeta(\boldsymbol{x}, t)$ and the free-surface potential $\varphi(\boldsymbol{x}, t) \equiv \Phi\big(\boldsymbol{x}, \zeta(\boldsymbol{x}, t), t\big)$ is in the Hamiltonian description given by the canonical equations

$$(2) \qquad \partial_t \zeta = +\rho^{-1}\, \delta\mathscr{H}/\delta\varphi \qquad \text{and} \qquad \partial_t \varphi = -\rho^{-1}\, \delta\mathscr{H}/\delta\zeta,$$

provided $\delta\mathscr{H}/\delta\Phi = 0$ in the fluid interior. In the remainder, we will consider just one horizontal coordinate x, but extension of the Hamiltonian model to two horizontal dimensions is straightforward. Next, to obtain a model depending only on x and t, the following assumption is made on vertical structure of the flow (see also Klopman *et al.*, 2005, 2007):

$$(3) \qquad \Phi(x, z, t) = \varphi(x, t) + f(z; h, \zeta, \kappa)\, \psi(x, t) \qquad \text{with} \qquad f(\zeta; h, \zeta, \kappa) = 0,$$

where $\psi(x, t)$ is an additional field to describe the non-uniformity of the interior fluid flow, *i.e.* its deviation from the shallow-water equations; $\kappa(x)$ is a parameter to be defined later on. In our approach it is essential to have $f = 0$ at the free surface $z = \zeta(x, t)$ in order to retain the Hamiltonian structure of the model. It is not needed to make assumptions regarding the non-linearity of the wave motion.
Apart from the canonical equations (2), we also have to solve $\delta\mathscr{H}/\delta\psi = 0$. Now, the components of the flow velocity become:

$$(4) \qquad \partial_x \Phi = \partial_x \varphi + f\, \partial_x \psi + \psi\, \partial_x f \qquad \text{and} \qquad \partial_z \Phi = \psi\, \partial_z f.$$

While in Klopman *et al.* (2005, 2007) we used a parabolic shape function $f(z;h,\zeta,\kappa)$, here we will use a hyperbolic cosine:

$$f = \left[\cosh\left(\kappa\,(z+h)\right) - \cosh\left(\kappa\,(\zeta+h)\right)\right] \,/\, N\big(\kappa\,(\zeta+h)\big), \tag{5}$$

where $N\big(\kappa(\zeta+h)\big)$ is a normalisation function, the choice of which has consequences on wave reflection to be studied later on. For example, the choice $N = \kappa\,\sinh\big(\kappa(\zeta+h)\big)$ results in ψ being the vertical velocity at the free surface, while with $N = 1$ we have that $\varphi+\psi$ is the velocity potential at the sea bed $z = -h(x)$. Furthermore, $\kappa(x)$ is the curvature parameter for the vertical structure, and we choose κ in such a way that $\kappa h(x)$ is determined from the linear dispersion relation $\omega^2 = g\kappa\,\tanh(\kappa h)$, using for the angular frequency ω some characteristic value.

Wave reflection will be studied for the case of linear waves. This is achieved by choosing the upper z-limit of the vertical integration of the Hamiltonian (1) to be zero. In the shape function (5), we also replace ζ with zero. A vertical integration yields the linear-theory Hamiltonian $\mathscr{H}_0(\zeta,\varphi;\psi)$:

$$\mathscr{H}_0 = \int \rho\left\{\tfrac12\,h\,(\partial_x\varphi)^2 + P\,(\partial_x\varphi)\,(\partial_x\psi) + X\,\psi\,\partial_x\varphi + Y\,\psi\,\partial_x\psi + \tfrac12\,K\,\psi^2 + \tfrac12\,F\,(\partial_x\psi)^2 + \tfrac12\,g\,\zeta^2\right\}\,\mathrm{d}x, \tag{6}$$

with the coefficients – functions of x through f depending on $h(x)$ and $\kappa(x)$ – given by:

$$P = \int_{-h}^{0} f\,\mathrm{d}z, \qquad F = \int_{-h}^{0} f^2\,\mathrm{d}z, \qquad X = \int_{-h}^{0} \partial_x f\,\mathrm{d}z, \tag{7a}$$

$$Y = \int_{-h}^{0} f\,\partial_x f\,\mathrm{d}z \qquad \text{and} \qquad K = \int_{-h}^{0}\left[(\partial_x f)^2 + (\partial_z f)^2\right]\mathrm{d}z, \tag{7b}$$

Using the canonical eqs. (2) and the constraint $\delta\mathscr{H}_0/\delta\psi = 0$, the model equations become:

$$\partial_t\zeta + \partial_x\left(h\,\partial_x\varphi + P\,\partial_x\psi + X\,\psi\right) = 0 \quad , \qquad \partial_t\varphi + g\,\zeta = 0 \qquad \text{and} \tag{8a}$$

$$K\,\psi - \partial_x\left(F\,\partial_x\psi + P\,\partial_x\varphi + Y\,\psi\right) + X\,\partial_x\varphi + Y\,\partial_x\psi = 0. \tag{8b}$$

In the last equation for the solution of ψ, one may be tempted to combine both terms containing $Y(x)$. However, at locations where there are discontinuities in the coefficients, continuity of the mass flux $h\partial_x\varphi + P\partial_x\psi + X\psi$ and the flux $F\partial_x\psi + P\partial_x\varphi + Y\psi$ is required. The form (8b) than may be advantageous, certainly when using a numerical approach retaining spatial conservative properties of the equations, such as *e.g.* a finite volume method.

For the hyperbolic-cosine shape function (5) (with ζ set to zero for this linear theory) we get the following coefficients, in case no normalisation is used ($N = 1$):

$$P^{(c)} = \frac{1}{\kappa}\left(\mathcal{S} - \kappa\,h\,\mathcal{C}\right), \qquad F^{(c)} = \frac{1}{\kappa}\left(-\frac32\,\mathcal{S}\,\mathcal{C} + \frac12\,\kappa\,h + \kappa\,h\,\mathcal{C}^2\right), \tag{9a}$$

$$X^{(c)} = \left(\mathcal{C} - 1 - \kappa\,h\,\mathcal{S}\right)\,h' + \frac{1}{\kappa^2}\left(-\,\mathcal{S} + \kappa\,h\,\mathcal{C} - \kappa^2\,h^2\,\mathcal{S}\right)\,\kappa', \tag{9b}$$

$$Y^{(c)} = \frac12\left[1 + 2\,\mathcal{C} - 3\,\mathcal{C}^2 + 2\,\kappa\,h\,\mathcal{S}\,\mathcal{C}\right]\,h' + \frac14\,\frac{1}{\kappa^2}\left[3\,\mathcal{S}\,\mathcal{C} + 3\,\kappa\,h\left(1 - 2\,\mathcal{C}^2\right) + 4\,\kappa^2\,h^2\,\mathcal{S}\,\mathcal{C}\right]\,\kappa', \tag{9c}$$

$$\begin{aligned} K^{(c)} = {} & \frac12\,\kappa\,(\mathcal{S}\,\mathcal{C} - \kappa\,h) + \kappa\left[\mathcal{S}\left(2 - \frac32\,\mathcal{C}\right) + \kappa\,h\left(\mathcal{S}^2 - \frac12\right)\right]\,(h')^2 \\ & + \frac{1}{\kappa}\left[\frac32\,\mathcal{S}^2 + \kappa\,h\,\mathcal{S}\left(2 - 3\,\mathcal{C}\right) + \kappa^2\,h^2\left(2\,\mathcal{S}^2 - \frac12\right)\right]\,\kappa'\,h' \\ & + \frac{1}{\kappa^3}\left[\frac14\,\mathcal{S}\,\mathcal{C} + \kappa\,h\left(\frac32\,\mathcal{S}^2 - \frac14\right) - \frac32\,\kappa^2\,h^2\,\mathcal{S}\,\mathcal{C} + \kappa^3\,h^3\left(\mathcal{S}^2 - \frac16\right)\right]\,(\kappa')^2, \end{aligned} \tag{9d}$$

with $\mathcal{S} \equiv \sinh(\kappa\,h)$ and $\mathcal{C} \equiv \cosh(\kappa\,h)$. Simplification of the resulting equations (8) may be obtained by using a mild-slope approximation, neglecting all x-derivatives of the shape function f in the integrand of the Hamiltonian $\mathscr{H}_0$. Consequently, for the hyperbolic-cosine shape function (5), we have the following coefficients in the mild-slope approximation:

$$P_m^{(c)} = \frac{1}{\kappa\,N}\left(\mathcal{S} - \kappa\,h\,\mathcal{C}\right), \qquad F_m^{(c)} = \frac{1}{\kappa\,N^2}\left(-\frac32\,\mathcal{S}\,\mathcal{C} + \frac12\,\kappa\,h + \kappa\,h\,\mathcal{C}^2\right), \tag{10a}$$

$$X_m^{(c)} = Y_m^{(c)} = 0, \qquad K_m^{(c)} = \frac{\kappa}{2\,N^2}\left(\mathcal{S}\,\mathcal{C} - \kappa\,h\right). \tag{10b}$$

Models resulting from coefficients (10) are called mild-slope models, while coefficients (9) lead to a so-called steep-slope model.

Optimisation of normalised mild-slope models During our research, it has been found that the normalisation of the shape function f has a large influence on the reflection coefficient. The advantage of the mild-slope models is that they are of simpler form than the corresponding steep-slope variants, even more in case of non-linear models. Instead of optimisation with respect to the accuracy of wave reflection in certain cases, we have chosen to minimize the steep-slope coefficient $X^{(co)}$ in (7) as a function of the normalisation $N(\kappa h)$. This, because in the resulting mild-slope approximation the coefficients $X_m^{(co)}$ and $Y_m^{(co)}$ are equal to zero. Our presumption is that by minimizing X, also Y and the slope-dependent terms in K will become small, and the resulting model will be close to the corresponding steep-slope model – a similar procedure for a model with a parabolic shape function showed that X, Y and additional terms in K indeed become very small. Consider the coefficient $X^{(co)}$. We replace κ' by the corresponding expression for h' using the linear dispersion relation. Then we have as a non-dimensional measure for $X^{(co)}$ the expression:

$$X^{(co)} = \left(\mathcal{S}\,\mathcal{C}\,\frac{(\kappa\,h\,\mathcal{C} - \mathcal{S})\,N'}{(\kappa\,h + \mathcal{S}\,\mathcal{C})\,N^2} - \frac{\mathcal{S}\,(\mathcal{C} - \mathcal{S}^2) + \kappa\,h\,(1 + \mathcal{S}^2\,\mathcal{C})}{(\kappa\,h + \mathcal{S}\,\mathcal{C})\,N} \right) \partial_x h. \tag{11}$$

By setting $X^{(co)}$ equal to zero, we obtain a differential equation for N in terms of $q \equiv \kappa h$, of which we

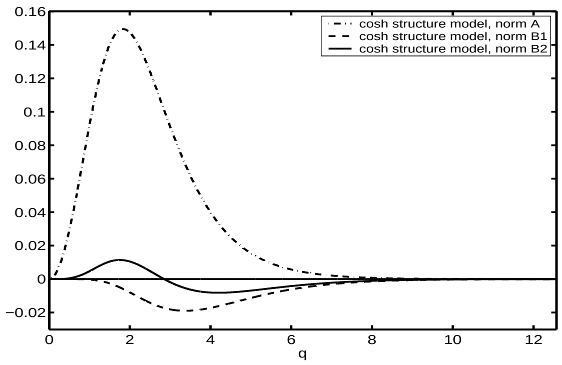

(a) Optimisation of the f–normalisation.

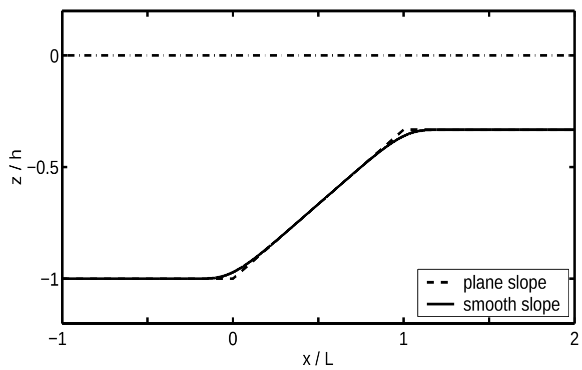

(b) Bathymetry.

FIGURE 1. (a) Variation of ν as a function of $q \equiv \kappa h$ for different normalisations of the shape function, Eq. (13). Dash-dot line: N_A; dashed line: N_{B_1}; solid line: N_{B_2}. (b) Bathymetry, for a plane slope (dashed line) and a smooth slope (solid line).

have not found an exact solution. In order to assess the performance of a normalisation, the following dimensionless quantity is used:

$$\nu = X^{(co)}\,h \,/\, \left(P^{(co)}\,\partial_x h\right), \tag{12}$$

which can be shown to be only a function of q. Although we have not been able to find analytic expressions for $N(q)$ which result in $\nu = 0$, we are able to find approximations to $N(q)$ which give small ν. Three different normalisations have been chosen which each have the correct asymptotic behaviour for $q \to 0$ and $q \to \infty$:

$$N_A = \sinh(q), \qquad N_{B_1} = \frac{3 + 37\cosh q}{13 + 27\cosh q}\sinh q \qquad \text{and} \qquad N_{B_2} = \frac{\sinh q\,\cosh q}{\frac{1}{4} + \frac{3}{4}\cosh q}. \tag{13}$$

Approximation N_A has the correct limiting behaviour for $q \to 0$ and $q \to \infty$. Approximation N_{B_1} is an improvement on this, using a Padé expansion for the remainder around $q = 0$, while N_{B_2} is a minimax approximation. The resulting $\nu(q)$ is shown in Figure 1(a).

Numerical results on reflection A plane slope of horizontal extent L, connecting two horizontal regions of constant depth h_1 for $x < 0$ and h_2 for $x > L$ (see Fig. 1), is used to study linear wave reflection by monochromatic waves of angular frequency ω. This test case was used by Booij (1983), with non-dimensional depths $k_\infty h_1 = 0.6$ and $k_\infty h_2 = 0.2$, where $k_\infty \equiv \omega^2/g$. The wave-amplitude reflection coefficient $|R|$ is computed over a range of relative slope lengths $k_\infty L$, and are compared with the highly-accurate numerical results of Porter & Porter (2006) for the full potential-flow problem. For a constant frequency ω, the model equations (8) transform into a set of ordinary differential equations for the complex-valued amplitudes of ζ, φ and ψ. This boundary-value problem is solved numerically using MATLAB-function *bvp4c*, using Sommerfeld weakly-reflective boundary conditions at locations far from the bends in the bed at $x = 0$ and $x = L$.

The resulting $|R|$ as a function of $k_\infty L$ for the mild-slope model (10) (without normalisation, $N = 1$) is

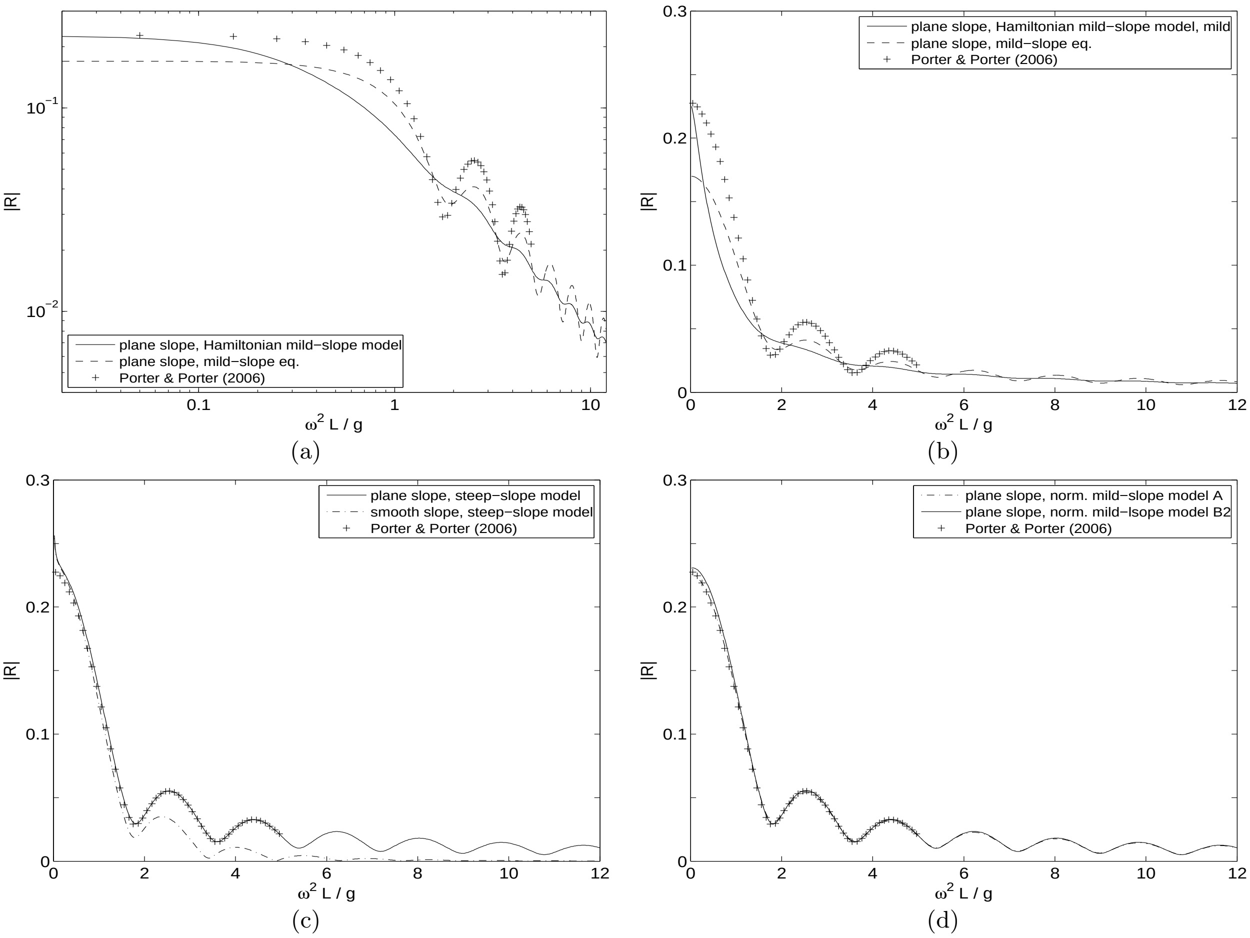

FIGURE 2. Reflection coefficient $|R|$ as a function of relative slope length $k_\infty L$.

shown in Fig. 2(a) and (b), on a double-logarithmic and a linear scale. Also the results for the classical mild-slope equation $\partial_x\big(cc_g\partial_x\eta\big) + k^2 cc_g\eta = 0$ are shown, with k the wave number according to the linear dispersion relation, while $c \equiv \omega/k$ and $c_g \equiv \partial\omega/\partial k$ are the phase and group speed, respectively. As can be seen, the oscillations in the reflection coefficient are not predicted well, by the mild-slope equation and even less by our unnormalised ($N = 1$) mild-slope model (10). Note that an important difference between the mild-slope equation and our ($N = 1$) mild-slope model is in the normalisation of the shape function. Next, Figs. 2(c) and (d) show that both the steep-slope model (9), as well as the mild-slope models with optimised normalisation N_A and N_{B_2}, see Eq. (13) give very good predictions of the reflection coefficient.

As already noted by Porter & Chamberlain (1997), the discontinuities in bed slope at $x = 0$ and $x = L$ in the Booij test case have a major effect on the reflections. Therefore, we also study a smooth slope, with the water depth varying in the interval $0 < x < \frac{1}{2}\pi L$ and given by:

$$h(x) = h_1 + \tfrac{1}{2}\,(h_2 - h_1)\,\left\{1 + \tanh\left[\tan\left(2\,x\,/\,L - \tfrac{3}{2}\,\pi\right)\right]\right\}. \tag{14}$$

This has the same maximum bed slope as the plain bed, while being continuous in the x-derivatives at all orders. As can be seen from Fig. 2(d), the smooth slope results in much less reflection for larger values of $k_\infty L$ (*i.e.* smaller bed slopes).

References

Booij, N. 1983. A note on the accuracy of the mild-slope equation, *Coastal Eng.* **7** (3), 191–203.

Klopman, G., Dingemans, M.W. & van Groesen, E. 2005. A variational model for fully non-linear water waves of Boussinesq type, *Proc. 20th IWWWFB*, Longyearbyen, Spitsbergen, Norway, May 2005.

Klopman, G., Dingemans, M.W. & van Groesen, E. 2007. Propagation of wave groups over bathymetry using a variational Boussinesq model, *Proc. 22th IWWWFB*, Plitvice, Croatia, April 2007.

Porter, D. & Chamberlain, P.G. 1997. Linear wave scattering by two-dimensional topography, In: *Gravity waves in water of finite depth*, Ed. J.N. Hunt, Adv. Fluid Mech. Ser. **10**, Comput. Mech. Publ., 13–53.

Porter, R. & Porter, D. 2006. Approximations to the scattering of water waves by steep topography. *J. Fluid Mech.* **562**, 279–302.

Zakharov, V. E. 1968. Stability of periodic waves of finite amplitude on the surface of a deep fluid. *J. Appl. Mech. and Techn. Phys.* **9**(2), 190–194.